Micro-patterning of Flexible and Free Standing Polyvinylidenedifluoride (PVDF) Films for Enhanced Pyroelectric Energy Transformation

D. Zabek[1], J. Taylor[2], E. LeBoulbar[1] and C. R. Bowen[1]

[1] Department of Mechanical Engineering, University of Bath, Bath, BA2 7AY, United Kingdom

[2] Department of Electrical and Electronic Engineering, University of Bath, Bath, BA2 7AY, United Kingdom

Corresponding author: D.Zabek@bath.ac.uk

Abstract:

In an effort to harvest thermal energy and exploit abundantly available waste heat the pyroelectric effect offers the opportunity to convert temperature fluctuations into useable electrical energy. This paper reports on the micro-patterning of the surface of a pyroelectric in order to enhance heat transfer and achieve faster and larger temperature fluctuations which improve pyroelectric energy transformation. Methods for the fabrication of partially covered electrodes on polyvinylidene difluoride (PVDF) films are developed to investigate and quantify the benefits of such an electrode structure for pyroelectric energy harvesting. The micro-pattern consists of an array of holes that are etched into the upper aluminium electrodes of free standing ferroelectric PVDF films using a low cost photo-lithography and wet etching process. Under the application of IR radiation heating, it is demonstrated that such micro-features are able to significantly improve the open circuit voltage by 380% and the closed circuit current by 420% for an electrode area coverage of 45% when compared to a fully covered electrode design. Capacitance measurements show constant electric fields with micro features for electrode area coverages as low as 28 %. A specific generator performance of 66.9 μJ cm^{-3} $cycle^{-1}$ is presented at oscillation temperatures of 2.8 °C.

Keywords: pyroelectric, energy harvesting, micro-pattern, flexible substrate, PVDF

1. Introduction

There is increasing demand for energy harvesting materials and systems for low power electronic applications such as sensors, antennas, wireless devices and networks or simply to recharge batteries [1]. The

ability to harvest local sources of energy enables systems, such as wireless sensors networks, to function autonomously and therefore significantly reduce operation and maintenance costs [2].

While spatial temperature gradients can be exploited using thermoelectric devices, temperature fluctuations can be harvested using generators employing pyroelectric materials. The use of pyroelectric materials is of interest since under the correct conditions they have the potential to operate with a high thermodynamic efficiency and power output, compared to thermoelectrics, since they do not require a spatial temperature gradient or particular geometry [3]. The origin of the pyroelectric effect stems from the presence of a dipole moment in a non-centre-symmetric crystal lattice and the fact that the level of polarisation *P (C m^{-2})* in a pyroelectric changes as a result of a change in temperature *dT (K)*. When the level of polarisation decreases on heating, surface bound charge become free and this creates an electric field across the polar axis. This potential difference can be discharged across an external load when the surface electrodes of the generator are interconnected. Under short circuit conditions, the pyroelectric current *I (A)* is [4]:

$$I = A.\frac{dP}{dT}.\frac{dT}{dt} = A.p.\frac{dT}{dt} \qquad (1)$$

for a given surface area *A (m^2)*, pyroelectric coefficient *p (C m^{-2} K^{-1})* and temperature change rate *dT/dt (K s^{-1})*. The effective pyroelectric current has been measured for convective heating on bulk lead zirconate titanate (PZT) and polyvinyliden-difluoride (PVDF) for a variety of geometries [5]. A different approach was conducted by Olsen et al. who introduced a thermodynamic cycle using applied electric fields for larger changes in polarisation[6].

From **Equation 1** there are two methods to increase the pyroelectric current generated by a device of a specific surface area. One approach is to increase *dT/dt*, which can be achieved by improving the heat transfer of the harvester [7]. In sensor applications, improvements in the generated current and voltage have been achieved by introducing a meshed or partially covered electrodes (PCE) on pyroelectric materials such as ZnO [8] and $LiTiO_3$ [9]. It has been shown that the replacement of a fully covered electrode with a partially covered electrode increases the thermal diffusion due to a higher radiation absorption coefficient of the pyroelectric material compared to the employed electrode material. For pyroelectric energy harvesting, Hsiao et *al*. adopted this approach using PZT where the temperature variation rate increases by 110 % compared to a fully covered electrode [10].

Another approach to enhance the pyroelectric current from **Equation 1** is to use materials with high pyroelectric coefficient since a wide range of pyroelectric materials are available for energy harvesting [6]. Hard, brittle and stiff ferroelectrics such as single crystal lead magnesium niobate-lead titanate (PMN-PT) and polycrystalline PZT exhibit high pyroelectric coefficients above 550 μC m^{-2} K^{-1}. In contrast, lightweight, low cost, lead free, tough and transparent polymeric materials such as semi-crystalline ~~polyvinyliden difluoride (~~PVDF~~)~~ exhibit a relatively low pyroelectric coefficient of 33 μC m^{-2} K^{-1} [7]. Materials with a nanoscale geometry haven been shown to exhibit a high pyroelectric coefficient of 68 μC m^{-2} K^{-1} in the form of a PVDF-TrFE copolymer as a dense nano-fibre array[11]. Despite the low pyroelectric coefficient of PVDF, the material has attracted attention for pyroelectric harvesting due to the high level of biocompatibility and mechanical flexibility, which makes it suitable for hybrid pyroelectric generators where the pyroelectric response is enhanced by the piezoelectric effect [12].

To date there have been no reports on methods for the fabrication of partially covered electrodes on PVDF films and an investigation of benefits of such an electrode structure for pyroelectric energy harvesting. In addition, PVDF is of great interest for hybrid piezo-pyroelectric wearable nano harvester devices since PVDF can be elastically deformed to high strains[13]. In this article we propose the use of aluminium partially covered electrode on PVDF as a simple and effective way to improve the energy generation capability of a pyroelectric energy harvester. **Figure 1** illustrates a square meshed partially covered upper electrode exposed to an infra-red (IR) radiation source.

The aim of the PCE is to considerably improve the heat absorption and temperature change since aluminium is highly reflective towards radiation whereas PVDF largely absorbs ~~infra-red~~ IR wavelengths above 700 nm [14]. When a pyroelectric film with a partially covered electrode structure is directly exposed to IR it has the potential to achieve higher absolute changes in temperature, higher rates of change in temperature and reduced reflections. We will first present the method of fabrication of partially covered aluminium electrodes with a particular small features size of ~~with~~ a (10 x 10) $μm^2$ square array on flexible and free-standing PVDF films. The second part of the paper will focus on the advantages of the partially covered electrode on the electrostatic properties of the film type device. Capacitance measurements, generated open-circuit voltage and closed-circuit current under constant IR illumination will be conducted and energy calculations will be presented as a function of electrode coverage.

Although the research presented is targeted to energy harvesting, the use of this micro-pattern is also directly applicable to others applications such as novel flexible and high resolution sensors, pressure sensor, skin for robotics or touchpad interfaces.

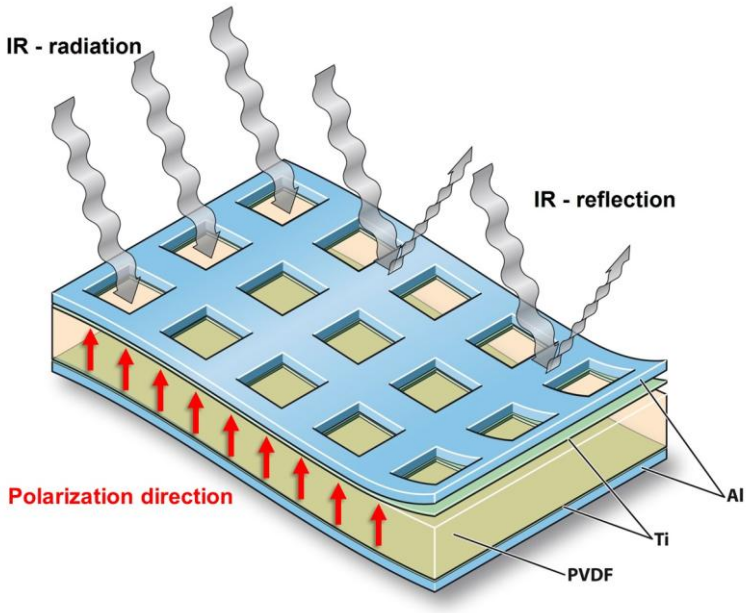

Figure 1: Pyroelectric generator with patterned top electrode exposed to IR radiation which is reflected at the aluminium electrode but absorbed at the exposed PVDF areas.

2. Experimental section

a. Fabrication of PCE

A pre-poled extruded 52 µm PVDF film (Precision Acoustics, UK) was used to manufacture the device for pyroelectric harvesting. Measurements by Fourier transformation infrared (FTIR) spectroscopy (see supplement **S1**) indicate the PVDF is in its β-phase and polarisation-field characteristics of the materials has been undertaken using an aixACCT PEES test system equipped with a TFAnalyzer 2000 and TREK 610E amplifier (see supplemental **S2** with a remnant polarisation of 6.78µC/m^2 and coercive field 776kV/cm). Since the PVDF is pre-poled condition, there is a need to preserve the ferroelectric and mechanical properties of the PVDF by limiting the number of manufacturing steps and ensuring each fabrication step has been carried out at temperatures of less than 60 °C. This is well below the maximum useable temperature for PVDF of 75 – 80 °C [15] ~~. ferroelectric to paraelectric phase transition temperature of PVDF [13]~~. Initially, ~~two~~a Ti (2 nm)/Al (200 nm) electrode~~s~~ was ~~were~~ deposited on ~~both~~one side~~s~~ of the pre-poled extruded PVDF film using a sequential electron beam vapour deposition system (Edwards FL-400) while maintaining the

temperature in the vacuum chamber below 38 °C. The 2 nm bonding layer of titanium was introduced in order to prevent pinhole generation, oxide formation, strip breaks, nano-cracks and to improve adhesion with the polymer film [16].

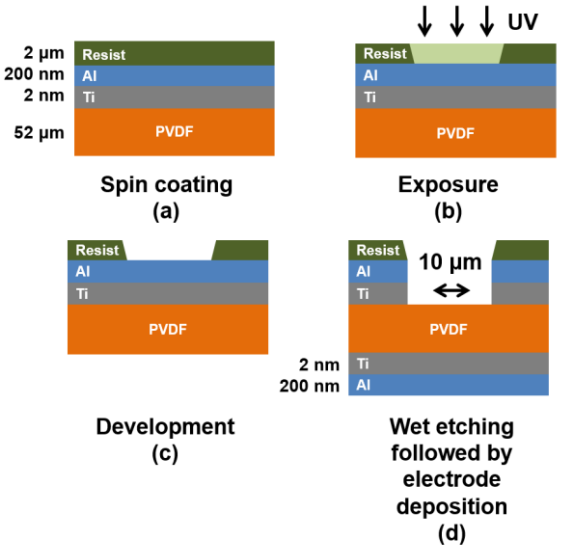

Figure 2: Manufacturing steps of micro-pattern on Al (200 nm)/Ti (2 nm)/PVDF pyroelectric harvester. (a) spin coating of photoresist (b) UV exposure of laser exposed micro-patterned surface (c) resist removal and development (d) wet etching of aluminium to expose PVDF followed by second electron beam vapour deposition of back electrode.

Micro-fabrication of meshed electrode was controlled using a direct laser writing process with a positive photoactive resist. Direct laser writing was employed since it is a versatile technique that allows exploration of a variety of electrode pattern geometries, fill factors and shapes. **Figure 2** is a schematic of the four main manufacturing stages, starting with the deposition of a 2 µm thick AS1512HS photoresist (MicroChemicals – Germany) layer by spin coating **(Figure 2a)**. The photoresist was spin coated at 50 s^{-1} and soft baked on a hot plate for 45 min at 55°C. The freestanding PVDF film was held on a carrier glass during the fabrication process in order to maintain flatness A direct laser writer (Heidelberg µPG 101 - Germany) was used to expose a (10 x 10) μm^2 square pattern array on a (2 x 1.5) cm^2 surface **(Figure 2b)**. The exposed photoresist was then dissolved in an AZ developer (MicroChemicals – Germany), revealing the aluminium surface and the remaining resist was hard baked for 30 min at 55°C **(Figure 2c)**. The exposed aluminium was then etched away by a wet etching process using an etchant solution (H_3PO_4:HNO_3:CH_3OOH:H_2O) for 2 minutes **(Figure 2d)**. The PVDF is reported to be resistant against these acids[15] and electron microscopy of a cross-

section reveals no damage of the PVDF (see supplemental **S3**). Finally, the remaining resist was removed with acetone and the PVDF film peeled off a handling ~~the~~glass substrate. The non-patterned backside of the device was electrode after etching using a second Ti (2 nm)/Al (200 nm) backside electrode electron vapour deposition **(Figure 2d).**

The electrode surface area was decreased by a gradual increase in the number of etched squares per total unit area so that devices with electrode coverages of 88, 70, 53, 45, 28 and 19 % were fabricated. **Figure 3** shows examples of the PCE mesh for surface area coverages of 70, 45 and 28%. A thick mesh with 70 % coverage has only two etched squares (**Figure 3a**) whereas a thin mesh with 28 % electrode coverage has around six etched squares for the same surface area of PVDF (**Figure 3c**). The uniformity of the etched square size as well as square quality was maintained constant for the total surface device area of (2 x 1.5) cm^2. This can be observed in the larger sections of the scanning electron microscopy images in the supplemental information (**S4**).

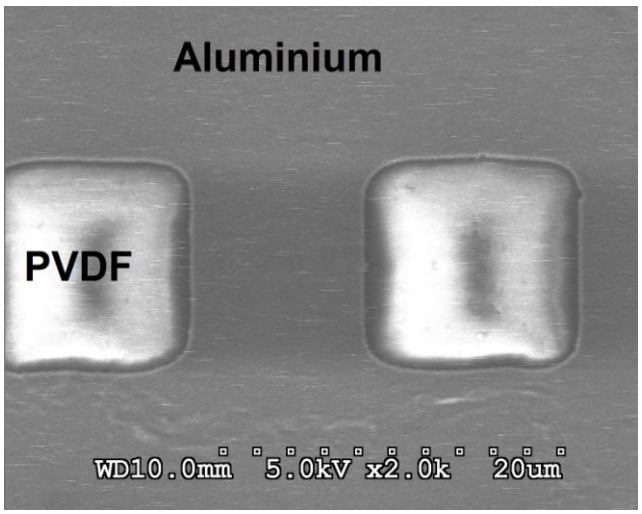

(a)

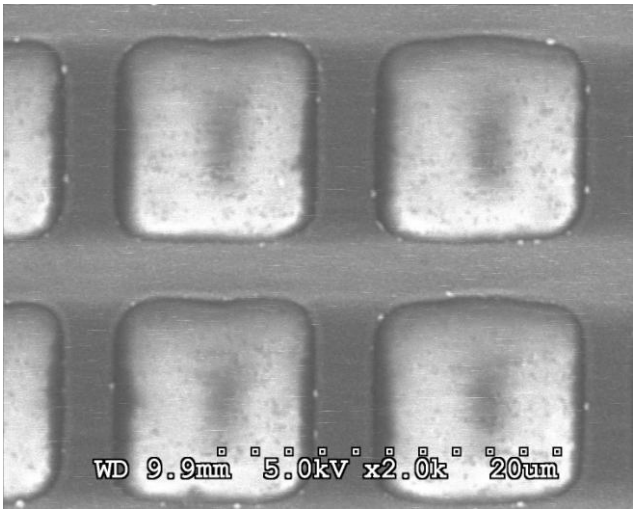

(b)

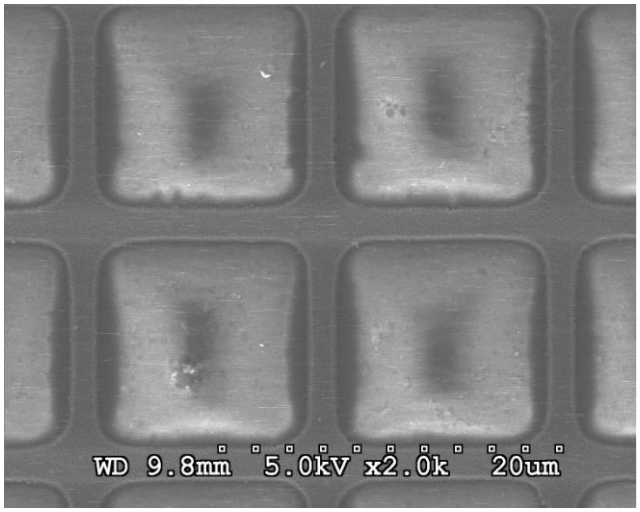

(c)

Figure 3: Examples of partially covered electrode with surface coverage of 70 (a), 45 (b) and 28 % (c). The light area is the aluminium electrode and darker area is the exposed PVDF.

b. Device characterisation

Since pyroelectrics are also dielectrics, the PVDF harvester configuration can be treated simply as an electrical insulator between two metal conductors. When heated under open circuit conditions, the released surface charge creates a potential difference across the electrodes, similar to a charged parallel plate capacitor. It is therefore of importance to characterise the device capacitance (C) as a function of partial covered electrode area in order to quantify the energy stored. For a parallel plate capacitor with a homogeneous electric field distribution between the capacitor areas (A) and the spacing (d) the capacity is:

$$C = \varepsilon_{33}^{T}.\varepsilon_0.\frac{A}{d} \qquad (2)$$

where ε_{33}^{T} is the relative permittivity of the PVDF ~~(ε_{33}^{T} = 10 – 12 [15])~~ at constant stress and ε_0 is the permittivity of free space (F m^{-1}). The capacitance of the devices and its dependency with electrode coverage was measured by a Solatron S1260 impedance analyser with a 1296 Dielectric Interface. Based on measurements of fully covered films a relative permittivity at constant stress of ε_{33}^{T} = 11 was calculated (supplemental information **S5**). **Figure 4** shows the measured capacitance of different electrode coverages for devices with identical geometry (2 cm x 1.5 cm x 52 µm). The measured capacitance (~600 pF) remains constant down to a 28 % PCE coverage. Further reductions in electrode coverages decrease the device capacity rapidly. This leads to the conclusion that the devices fabricated have the ability to maintain the electric field with PCE coverage of over 28 %.

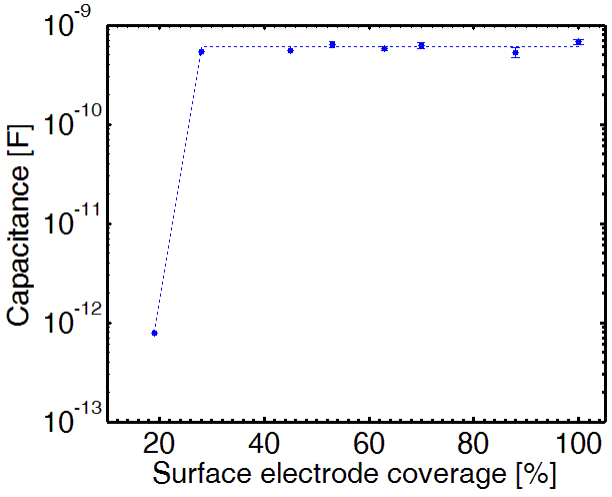

Figure 4: Capacitance measurements for different surface electrode coverage.

Due to the thin geometry (high surface to thickness ratio) of the device with etched squares the potential difference cerates fringing electric fields, which are predominant along the micro pattern [16]. The electric field E (V m^{-1}) and the open circuit voltage V is:

$$V = E.d = \frac{p}{\varepsilon_{33}^{T}}.d.\Delta T \qquad (3)$$

Since the specific stored energy Q ($J\ m^{-3}$) in a capacitor is ½ CV^2, this leads to:

$$Q = \frac{1}{2}.\frac{C}{A.d}.V^2 = \frac{1}{2}.\frac{p^2}{\varepsilon_{33}^{T}}.(\Delta T)^2 \qquad (4)$$

for a particular device thickness and developed change in temperature.

3. Temperature and electric energy measurements

Controlled temperature oscillations were applied to the patterned devices to assess the pyroelectric short circuit peak current and open circuit peak voltage for different PCE designs. Supplemental information **S6** provides a picture of the manufactured film type harvester. Seven PCE harvesters with a range of electrode coverage were placed ~~directly~~ 15 cm below a 175 W IR light bulb. When the light was switch on, the exposed device was heated and when the light is switched off, free convection led to device cooling (room temperature of 22 °C). Temperatures were captured when the average temperature for a switching frequency of 0.05 Hz were stable so that the energy balance aggregates to zero for radiative lamp heating and convective cooling, neglecting other heat transfer phenomena. The developed temperature of the PCE samples was measured at a sampling rate of 10 sec^{-1} using a K-Type thermocouples at the surface of the PVDF film by contact conduction. The thermocouple was electrically insulated from the PVDF with a thin coating of lacquer. Short circuit current and open circuit voltage was measured using a Keithley (US) 6514 electrometer. The corresponding rate of change of temperature dT/dt was calculated using the time forward derivative.

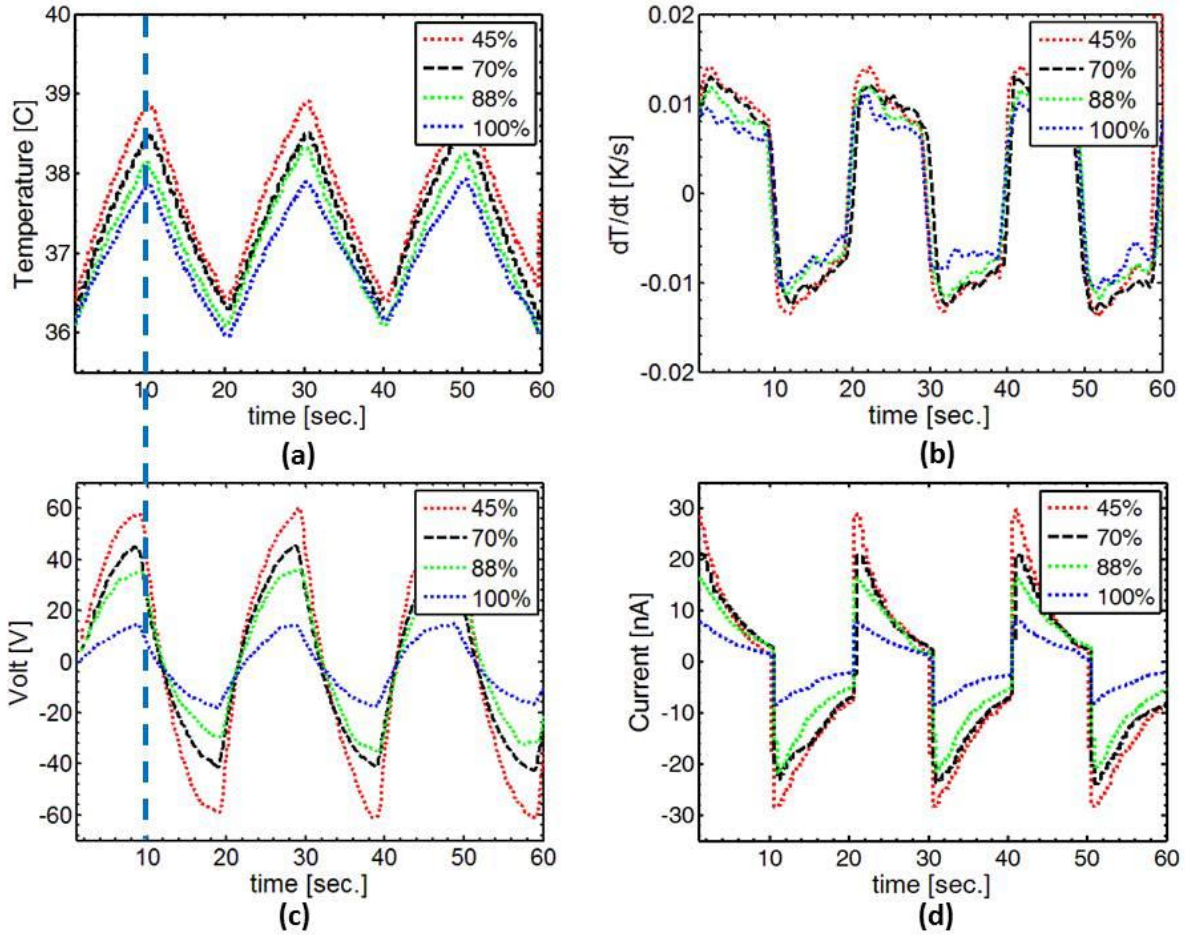

Figure 5: Developed (a) temperature, (b) rate of change of temperature, (c) open circuit voltage, (d) closed-circuit current for 100, 88, 70 and 45 % electrode coverage at temperature oscillation of 0.05 Hz.

Figure 5a shows temperature variation with time for PVDF with different electrode coverage, along with a fully covered electrode for comparison. From **Figure 5a** it can be observed that the absolute temperature magnitude (T) and its difference (ΔT) becomes larger with decreasing surface electrode coverage. The temperature profile for a 70 % PCE shows a 2.2 °C change in temperature over 10 seconds while 45 % PCE results in a larger change in temperature of 2.8 °C. For identical boundary conditions, the fully covered (100%) sample temperature changes by only 1.5 °C. By measuring the developed temperature over the full range of electrode coverage (100, 88, 70, 53, 45, 28 and 19 %), it was observed that when the PCE coverage decreases, the rate of change of temperature, dT/dt, also increases. According to **Equation 1**, faster rates of change in temperature **(Figure 5b)** lead to a larger closed circuit currents. Particularly for the early portion of each wave the difference in dT/dt between a patterned and unpattern harvester is larger. Subsequently, corresponding current measurements in **Figure 5d** confirm the ability to increase the closed circuit current by decreasing the electrode coverages. As an example, the 70 % covered electrode has a closed circuit

pyroelectric current of 20 nA and when compared to the fully covered electrode that develops 7 nA for identical conditions, the enhancement in heat transfer improves the closed circuit current by 285 %. Considering the corresponding open circuit transient voltage response, a larger temperature change leads to a higher voltage according to **Equation 3**. In **Figure 5c**, the 70 % PCE develops a closed circuit voltage of 42 V which is an increase of 280% compared to the 16 V for the fully covered reference sample.

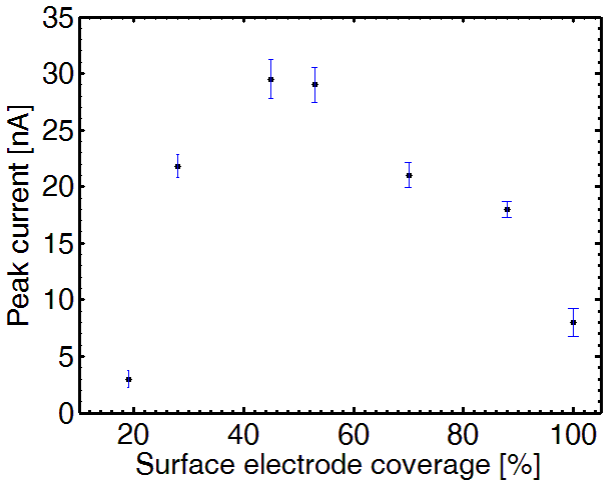

(a)

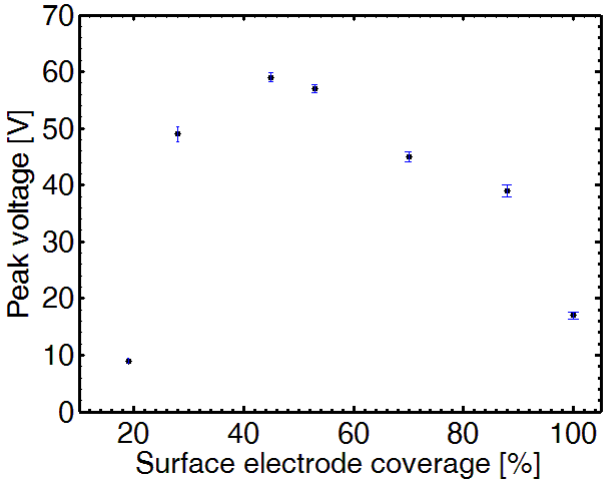

(b)

Figure 6: Measured peak (a) closed circuit current (b) open circuit voltage for a range of surface electrode coverages.

Clearly the higher heating and diffusion rates associated with a PCE lead to faster thermally induced changes in polarisation and developing more released charge at the electrode surface followed by a higher energy transformation. **Figure 6a** shows the pyroelectric short-circuit current and **Figure 6b** open-circuit voltage for the whole range of electrode areas examined. For a 45 % PCE a peak current of 30 nA and a peak voltage of 59 V is achieved and when compared to a fully covered electrode reference sample with a current of 8 nA and a voltage of 16 V, the 45 % PCE provides a 380% higher voltage and a 420% higher current. The optimization approach shows a local maximum at 45 % for the energy transformation so that further decrease in PCE coverage leads to a deterioration of generated pyroelectric current and voltage. Ultimately the optimum PCE is a balance between the area of electrically conductive aluminium required to collect the

free charges to the exposed PVDF area to improve heat transfer. Supplement **S6** shows a cross section view of a PCE harvester with a patterned top electrode and a continuous bottom electrode.

Considering a 59 V peak voltage for the 45 % PCE and a measured capacitance of 600 pF, the energy stored in the pyroelectric element is 1.04 μJ. On a volumetric basis, the energy density is 66.9. μJ cm^{-3} per thermal cycle. Finally, due to the squared relation of energy and voltage, the 45 % PCE has a 1080 % higher energy transformation than the fully covered reference, which only provides 6.2 μJ cm^{-3} $cycle^{-1}$. . In addition, the generated energy of the patterned device corresponds to a harvesting effectiveness k^2 of 0.19 % for a volumetric heat capacity of 1.8 J m^{-3} K^{-1}, relative permittivity ε_{33}^{T} = 11, pyroelectric coefficient of 33 μC m^{-2} K^{-1} and source temperature of 39 °C[17].

The 66.9 μJ cm^{-3} of micro-patterned PVDF is smaller than a measured energy density of 420 μJ cm^{-3} for PZT at approximately 42.5 °C with a fully covered electrode; this is associated with the significantly higher pyroelectric coefficient of PZT compared to PVDF [18]. Measurements on a PMN-PT single crystal show pyroelectric energy densities of 149 mJ cm^{-3} at temperatures slightly above room temperature [17]. Both PZT and PMN-PT are high stiffness and brittle ceramic materials, therefore the improvements associated with micro-patterned PVDF apporach provides a route for flexible and low cost pyroelectric harvesters; the energy density could be further improved using a PVDF-TrFE copolymer [11].

4. Conclusions

This paper reports that a simple modification of the electrode design to employ a partially covered electrode enables a significant increase in pyroelectric voltage (380 %), current (420 %) and pyroelectric energy harvesting transformation (1080 %). A low cost photo-lithography and wet etching process has been developed which allows the concept of a PCE to be readily up-scalable and geometry independent. It has been demonstrated that the optimum electrode area coverage for harvesting is achieved by balancing the area fraction of electrically conductive aluminium required to collect the free charge to the area fraction of exposed PVDF to improve heat transfer. The use of a partially covered electrode on PVDF thin films provides scope to widen the range of potential energy harvesting applications due to the beneficial material properties of flexibility, toughness and ease of fabrication as free-standing films. Compared to existing research conducted in this field, our approach is the first to be directly applicable to wearable devices, novel

flexible sensors, nano-scale devices and large scale pyroelectric energy harvesters due to its free-standing and cost effective nature. Future work will focus on smaller PCE features for higher and faster radiation absorption. In addition, the impact of PCE for conduction and convection needs to be assessed to broaden the range of potential heat transfer improvements.

Acknowledgements

We would like to acknowledge funding from the European Research Council under the European Union's Seventh Framework Programme (FP/2007–2013)/ERC Grant Agreement no. 320963 on Novel Energy Materials, Engineering Science and Integrated Systems (NEMESIS).

References

1. K. Ling Bing, Li, T., Hng, H.H., Boey, F., Zhang, T., Li, S.: 'Waste Energy Harvesting', 592; **2014**, Springer.
2. S. Beeby and N. White: 'Energy harvesting for autonomous systems', 308; **2010**, Norwood (USA), Artech House.
3. G. Sebald, D. Guyomar, and A. Agbossou: 'On thermoelectric and pyroelectric energy harvesting', *Smart Materials and Structures*, **2009**, 18(12), 125006.
4. S. B. Lang: 'Sourcebook of pyroelectricity', XV, 562 S.; **1974**, London u.a., Gordon and Breach.
5. A. Cuadras, M. Gasulla, and V. Ferrari: 'Thermal energy harvesting through pyroelectricity', *Sensors and Actuators A: Physical*, 2010, **158**(1), 132-139.
6. R. B. Olsen, D. A. Bruno, and J. M. Briscoe: 'Pyroelectric conversion cycles', *Journal of Applied Physics*, 1985, **58**(12), 4709-4716.
7. M. Suen, D. T. Lin, Y. Hu, and J. Hsieh: 'A Numerical Study of the Heat Transfer Phenomena on ZnO Pyroelectric Film Sensor', Proceedings of the International MultiConference of Engineers and Computer Scientists, **2010**.
8. C. S. Wei, Y. Y. Lin, Y. C. Hu, C. W. Wu, C. K. Shih, C. T. Huang, and S. H. Chang: 'Partial-electroded ZnO pyroelectric sensors for responsivity improvement', *Sensors and Actuators A: Physical*, **2006**, 128(1), 18-24.
9. V. Norkus, A. Schulze, Y. Querner, and G. Gerlach: 'Thermal effects to enhance the responsivity of pyroelectric infrared detectors', *Procedia Engineering*, **2010**, 5(0), 944-947.
10. C.-C. Hsiao, J.-C. Ciou, A.-S. Siao, and C.-Y. Lee: 'Temperature Field Analysis for PZT Pyroelectric Cells for Thermal Energy Harvesting', *Sensors*, **2011**, 11(11), 10458-10473.
11 L. Persano, C. Dagdeviren, Y. Su, Y. Zhang, S. Girardo, D. Pisignano, Y. Huang, and J. A. Rogers: 'High performance piezoelectric devices based on aligned arrays of nanofibers of poly(vinylidenefluoride-co-trifluoroethylene)', *Nat Commun*, 2013, **4**, 1633.
12. C. R. Bowen, J. Taylor, E. LeBoulbar, D. Zabek, A. Chauhan, and R. Vaish: 'Pyroelectric materials and devices for energy harvesting applications', *Energy & Environmental Science*, **2014**.

13. J.-H. Lee, K. Y. Lee, M. K. Gupta, T. Y. Kim, D.-Y. Lee, J. Oh, C. Ryu, W. J. Yoo, C.-Y. Kang, S.-J. Yoon, J.-B. Yoo, and S.-W. Kim: 'Highly Stretchable Piezoelectric-Pyroelectric Hybrid Nanogenerator', *Advanced Materials*, 2014, **26**(5), 765-769.

14. X. Li, S.-G. Lu, X.-Z. Chen, H. Gu, X.-s. Qian, and Q. M. Zhang: 'Pyroelectric and electrocaloric materials', *Journal of Materials Chemistry C*, **2013**, 1(1), 23-37.

15. Precision-Acoustics-Ltd.: 'PVDF properties and uses', **2013**, Dorset.

16. O. Keles and M. Dundar: 'Aluminum foil: Its typical quality problems and their causes', *Journal of Materials Processing Technology*, **2007**, 186(1–3), 125-137.

17. G. Sebald, E. Lefeuvre, and D. Guyomar: 'Pyroelectric energy conversion: Optimization principles', *Ultrasonics, Ferroelectrics, and Frequency Control, IEEE Transactions on*, 2008, **55**(3), 538-551.

18. Q. Zhang, A. Agbossou, Z. Feng, and M. Cosnier: 'Solar micro-energy harvesting with pyroelectric effect and wind flow', *Sensors and Actuators A: Physical*, 2011, **168**(2), 335-342.

Highlights:

- Novel PVDF energy harvesting material based on partially covered electrode
- Fabrication of high quality partially covered electrodes on PVDF films with 10 μm features size
- Enhancement in pyroelectric voltage (380 %), current (420 %) and pyroelectric energy harvesting transformation (1080 %).
- Cost effective and simple approach to pyroelectric enhancement

Supplemental 1:

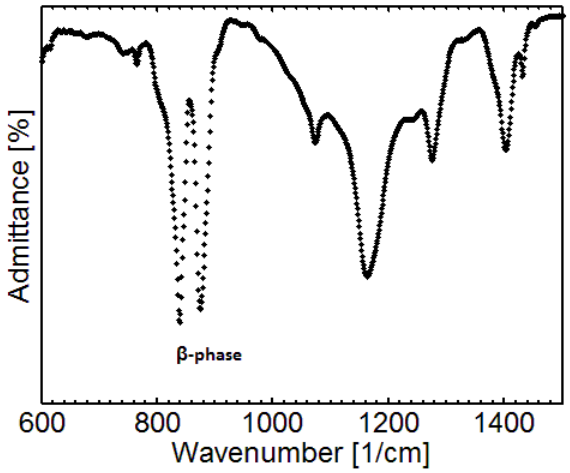

S1: Fourier transformation infrared spectroscopy (FTIR-ATR) with PerkinElmer Frontier (USA) of the employed ferroelectric PVDF film.

Supplemental 2:

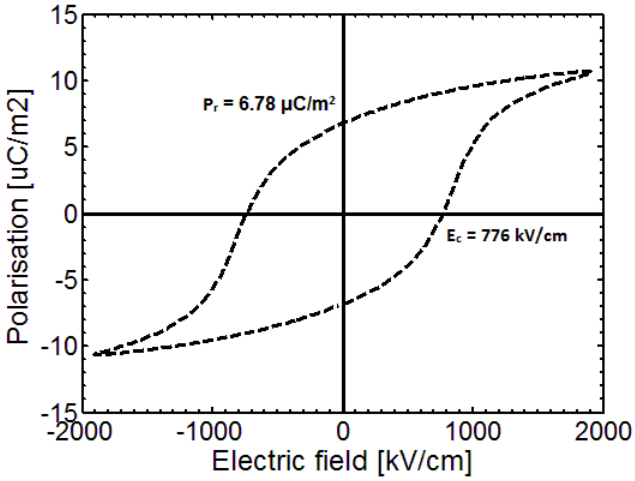

S2: Polarisation-field loop for the employed ferroelectric PVDF film measured using an aixACCT PES test system. The sample was immersed in Dow Corning silicone fluid during test. A 1 Hz 10 kV triangle waveform was used to record the PE loops. Remnant polarisation (P_r) and coercive field (E_c) indicated.

Supplemental 3:

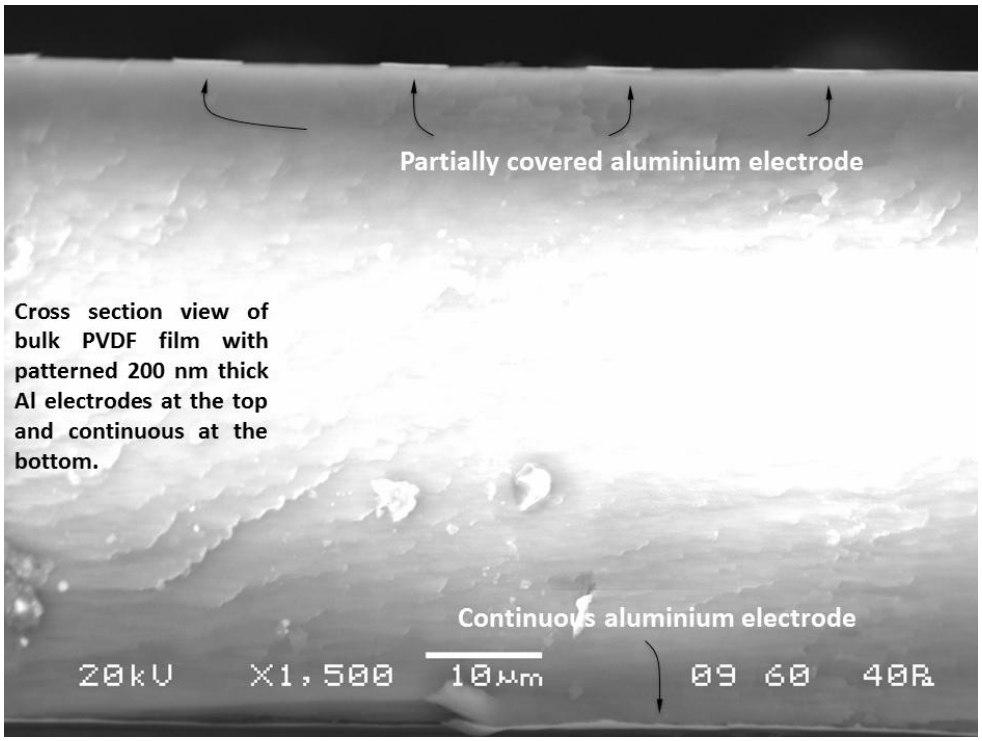

S3: Cross section view of patterned PVDF.

Supplemental 4:

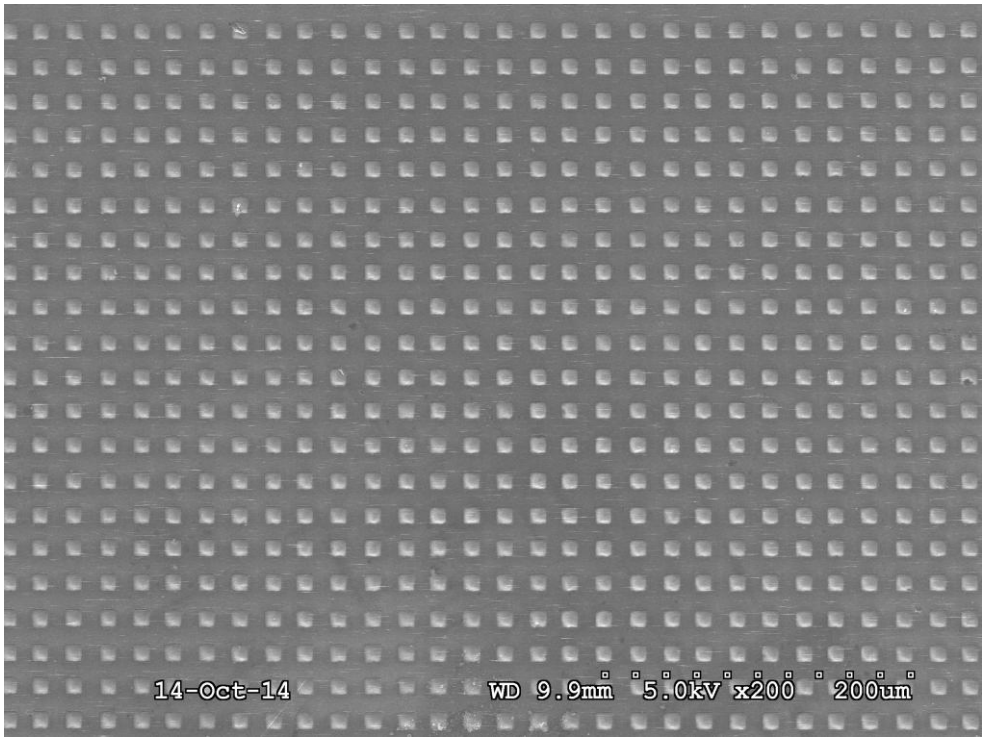

(70 %)

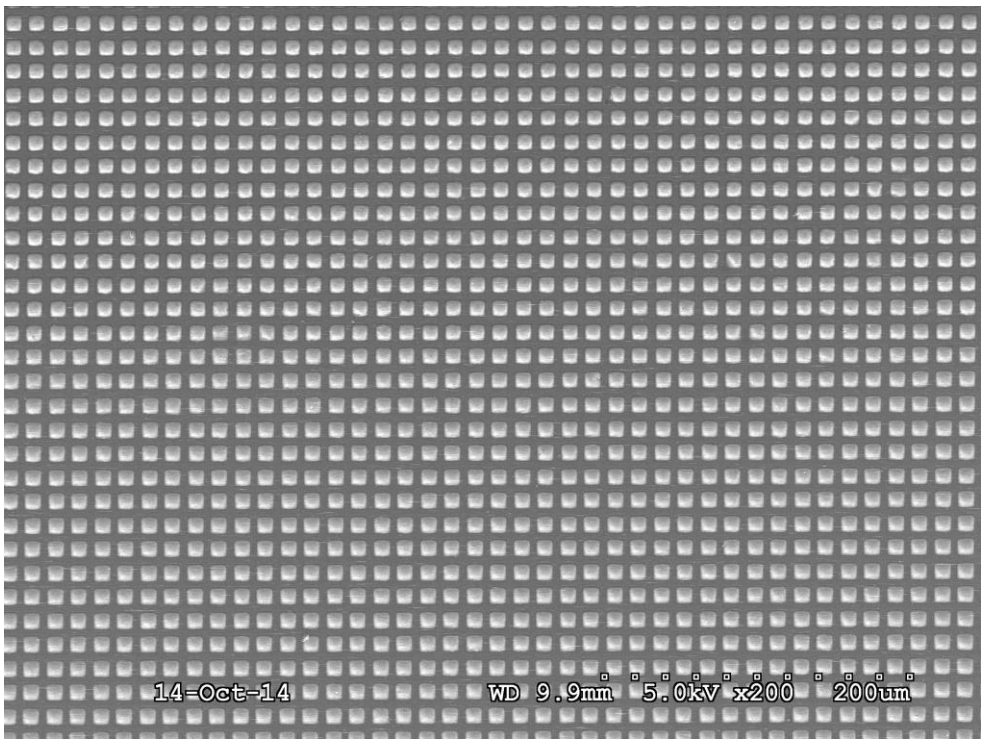

(45 %)

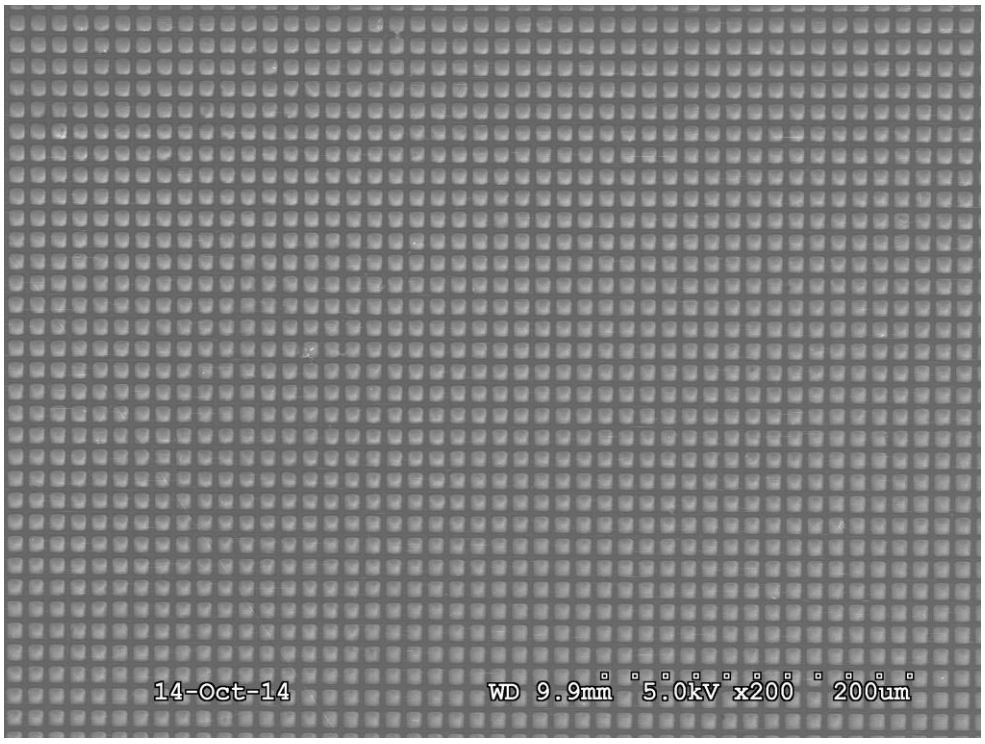

(28 %)

S3: SEM picture of 70 %, 45% and 28 % coverage of partially covered PVDF showing long range uniformity, quality of film, no cracking.

Supplemental 5:

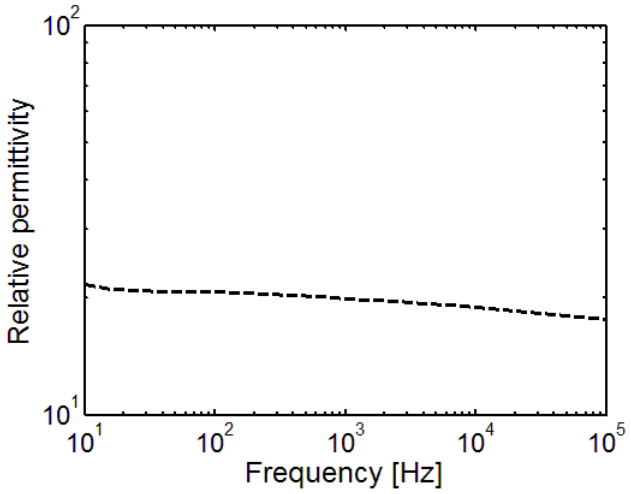

S5: Measured relative permittivity versus frequency from capacitance fully covered electrode sample.

Supplemental 6:

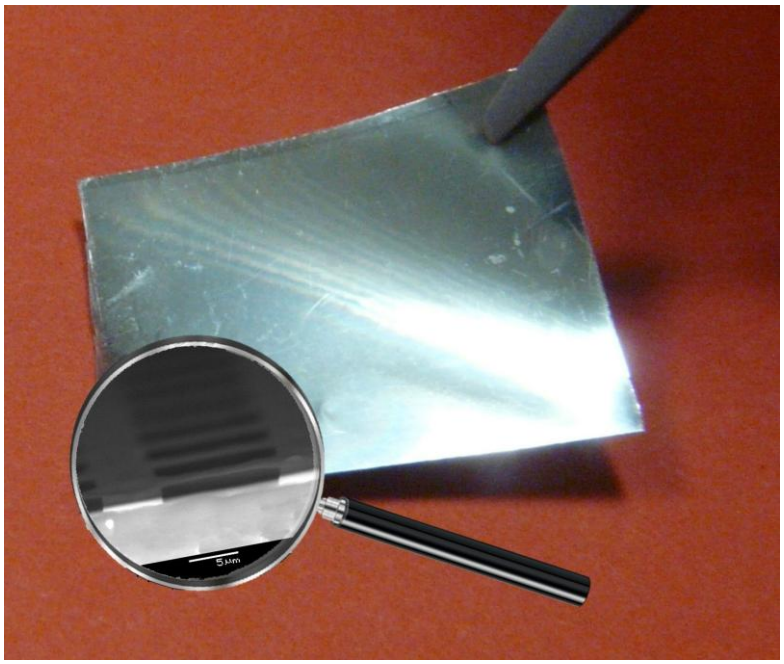

Supplemental 6: Image of the pyroelectric device.

Production Data

Click here to download Production Data: REVISED_manuscript_AEM - Copy.docx